A Solid-State Atomic Frequency Standard

Christopher J. White and Ali Hajimiri
Dept. of Electrical Engineering
California Institute of Technology
1200 E. California Blvd., MS 136-93, Pasadena, CA 91125
Email: cjwhite@caltech.edu

Abstract—**This paper describes a new class of frequency reference. The frequency source uses the same operating principle as a passive atomic frequency standard; however, the device is entirely solid-state, removing many cost and reliability issues associated with gas phase atomic clocks. More specifically, the "atomic resonance" is derived from zero-field magnetic resonance transitions of the vanadium ion in magnesium oxide. The characteristics of these resonances will be described in detail. The apparatus for measuring the "atomic" resonances uses a microwave resonant cavity and frequency-discriminator circuit. Using integrated circuits, the radio-frequency signal processing functions can be implemented at very low cost in a reliable manufacturing process. We discuss the system design and the measurement sensitivity. The estimated short term stability is in the range of 10^{-8} to 10^{-9} @ 1 s. Advantages of the new frequency reference may include immunity to vibration, reduced aging compared to crystal oscillators, and immediate cold start.**

I. INTRODUCTION

Crystal oscillators and atomic clocks are the two basic classes of frequency standards, and differ widely on their accuracy, size, cost, and power requirements [1]. Historically, the mainstream applications of crystal oscillators have been very different from atomic clocks. Most atomic clocks were used in laboratories for making highly precise measurements, or maintaining the basic standard of time. Recent trends in frequency standards have been to aggressively shrink the size of rubidium atomic clocks and to develop batch manufacturing techniques to lower the production cost in volume [2-12]. Every possible refinement has been applied to improve the long-term accuracy and temperature stability of crystal oscillators [13-18], and to reduce the power consumption of oven-controlled devices [19-23]. Warm-up time is an important feature of both technologies, which limits the use of precision frequency control in battery powered systems and tactical applications. For rubidium references, the absorption cell must be heated to reach adequate vapor pressure to operate the clock [24].

We propose a new class of frequency reference which may be manufactured at very low-cost using standard techniques. Short-term stability in the range of 10^{-8} to 10^{-9} at 1 second can be easily demonstrated with development of the new technology. The new frequency reference may prove to have better aging, retrace, and vibration sensitivity characteristics than crystal oscillators, immediate cold start, and possibly reduced sensitivity to space radiation [25].

II. PRINCIPLE OF OPERATION

The principle of operation of the solid-state atomic frequency reference is similar to other microwave passive atomic frequency standards. The difference is in the implementation of the atomic resonator and the detection technique used to interrogate the "atomic" resonance. In contrast to conventional atomic clocks using alkali metal gases, the "atomic" resonator consists of paramagnetic ions doped into a dielectric crystal. The solid-state hyperfine resonance is measured directly via the resonant change in the magnetic susceptibility of the sample.

Many atomic clocks use a simple integrator to lock the voltage-controlled oscillator to the atomic resonance signal (Figure 1):

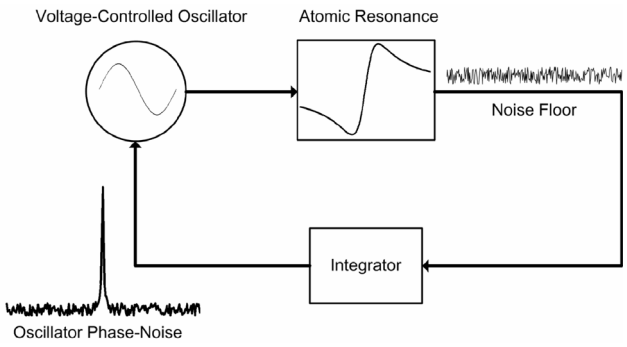

Figure 1. Microwave Passive Atomic Frequency Standard

Assuming the short-term stability of the passive atomic frequency standard is due to a white noise process, the Allan deviation is given by:

0-7803-9052-0/05/$20.00 © 2005 IEEE.

$$\sigma_{y,A} = \frac{1}{\sqrt{2}} \frac{\sqrt{S_n}}{f_A \left(\frac{\partial E}{\partial f} \right)} \tau^{-1/2} \qquad (1)$$

In Equation 1, S_n is the power spectral density of the measurement noise floor, $\delta E/\delta f$ is the slope of the atomic resonance measurement signal, f_A is the frequency of the atomic resonance, and τ is the integration time for the Allan deviation. To achieve good short term stability, we need a narrow atomic resonance (i.e., high-Q_A) and a high sensitivity measurement. Thus, the first major problem is to identify a materials system in solid-state which exhibits narrow hyperfine resonances, and to determine a suitable measurement technique to interrogate this resonance.

III. Solid-State Hyperfine Resonances

The first major question was whether we could find a solid-state materials system which would exhibit narrow hyperfine resonances at room temperature. The most interesting types of compounds are dielectric crystals doped with transition metal ions, where many interesting paramagnetic resonance properties arise because of the unpaired *d*-shell electrons which are weakly bonded to the host crystal [26-29]. Paramagnetic resonance may be measured at room temperature for certain combinations of crystal symmetry and impurity valance state. In particular, divalent vanadium in magnesium oxide has a spin Hamiltonian very similar to the Hamiltonian describing the hyperfine structure of an alkali metal atom [30, 31]:

$$\mathrm{H} = g_S \mu_B \mathbf{S} \cdot \mathbf{H} + A \mathbf{S} \cdot \mathbf{I} \qquad (2)$$

In Equation 2, A is the hyperfine constant, S is the spin of the electrons (S = 3/2 for V^{++}), I is the spin of the nucleus (I = 7/2 for vanadium), g_S is the electron Landé g-factor ($g_S \sim 2$ for V^{++}/MgO), μ_B is the Bohr magneton, and H is the applied magnetic field. The hyperfine constant A is approximately 80.3 Gauss (i.e., 225 MHz) [30, 31]. The analysis presented here does not consider much smaller S^3 terms in the complete Hamiltonian [32].

The vanadium spin Hamiltonian (2) is similar to the spin Hamiltonian which describes the hyperfine interaction for the S-orbital valence electron of an alkali metal vapor. Several important results, such as the existence of magnetic field independent transitions, are features of the spin Hamiltonian (2). The hyperfine structure of V^{++}/MgO is plotted in Figure 2, where the zero-field energies correspond to eigenstates F = 2, 3, 4, and 5. There are $2F + 1$ Zeeman levels in each F manifold corresponding to the eigenvalues $m_F = \{F, F-1, F-2, \ldots, -|F-1|, -F\}$. Using the Landé interval rule, the allowed transition frequencies at zero-field are at frequencies 3A, 4A, and 5A, i.e., ~500 MHz, 900MHz, and 1125 MHz. The measurement results presented below are for the F = 4 to F = 5 transitions at ~1125 MHz.

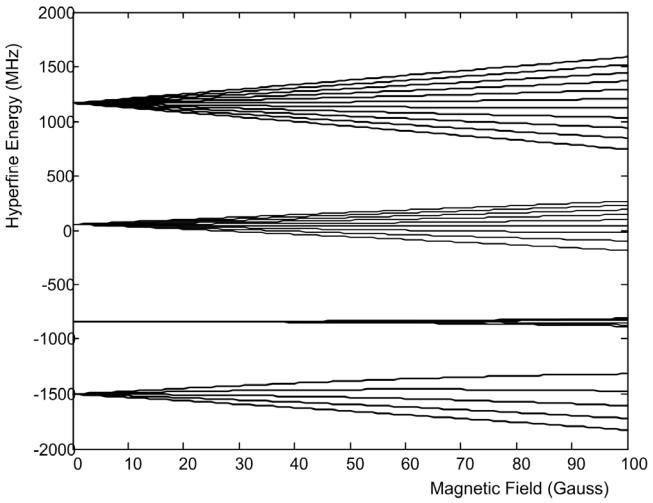

Figure 2. Hyperfine Structure for V^{++}/MgO

The Zeeman shift of a resonance line is determined by the Landé factors g_F and the quantum numbers m_F of the initial and final states [33,34], and for transitions of the type

$$\left| F = 4, m_F \right\rangle \leftrightarrow \left| F = 5, m_F \right\rangle . \qquad (3)$$

is equal to

$$\frac{1}{10} g_S \hbar \cdot m_F = (0.28 MHz / G) \cdot m_F . \qquad (4)$$

In Figure 2, the exact eigenvalues are used from a numerical solution to (2) at each value of the applied magnetic field **H**. The second-order Zeeman shift is evident at magnetic fields above approximately 50 Gauss. For Zeeman fields from 0 to 20 Gauss, the first-order theory is a close approximation to the exact solution.

IV. Experimental Arrangement

The second major question was to determine the best experimental technique to interrogate the solid-state hyperfine resonances. Initially, we considered the possibility of using optical pumping techniques similar to gas phase atomic clocks, but found that direct detection of the resonance in the magnetic susceptibility of the paramagnetic sample was the simplest and most sensitive technique.

A. Zero-Field Paramagnetic Resonance

The magnetic susceptibility of an MgO sample doped with paramagnetic V^{++} ions due to the $m_F = 0$ to $m_F = 0$ transition between the F = 4 and F = 5 energy levels is [34, 35]:

$$\chi''(\upsilon) = \frac{5775}{99000} \cdot \frac{2(g_S \mu_B)^2}{kT} \cdot \frac{N}{32} \cdot \frac{\Delta\nu\nu_0}{(\nu - \nu_0)^2 + (\Delta\nu/2)^2}. \qquad (5)$$

In Equation (5), g_S is the electron g-factor, μ_B is the Bohr magneton, k is Boltzman's constant, T is the absolute temperature, N is the concentration of paramagnetic ions, ν_0 is the paramagnetic resonance frequency, and $\Delta\nu$ is resonance width. Evaluating the constant factors, and assuming a magnesium oxide crystal doped with 100 ppm V^{++} relative to the anion lattice is (in CGS units):

$$\chi''(\upsilon) = 1.62 \times 10^{-10} \cdot \frac{\Delta\nu\nu_0}{(\nu - \nu_0)^2 + (\Delta\nu/2)^2} \qquad (6)$$

For example, if the transition frequency is 1114 MHz and the resonance width is 1MHz, the magnetic susceptibility on resonance is 0.72×10^{-6}.

In practice, the main difficulty in verifying (6) is in determining the number of vanadium ions which substitute into the lattice in the correct valence state. Vanadium ions tend to be incorporated in the trivalent state in as-grown crystals [31,36-38]. Transition metal dopants may also form precipitates in magnesium oxide, depending on the fabrication technique and heat treatment history, which has sometime resulted in confusion in the EPR literature on magnesium oxide [39]. In particular, one author was unable to reproduce results on linewidth broadening vs. concentration on account of the formation of ferrimagnetic precipitates [40].

Single crystal MgO samples with nominal vanadium doping of 450 ppm were obtained from Escete (Enshede, The Netherlands). The samples were annealed for 6 hours at 1100ºC in a reducing atmosphere (Ar/H_2), which increased the amount of divalent vanadium by at least an order of magnitude, as determined from X-band EPR measurements [34]. In general, single crystal samples are not needed, and the same results may be obtained using ceramic MgO.

B. Loop-Gap Resonator

The previous sections have described the physics of zero-field paramagnetic resonance with little reference to the experimental techniques used to measure zero-field magnetic resonance, or the practical design of a solid-state atomic frequency standard. The most important articles which described the design of zero-field paramagnetic resonance spectrometers are Delfs and Bramley [41,42] and Bramley and Strach [43,44]. Some early spectrometers detect the change in attenuation or phase along a non-resonant transmission line containing the paramagnetic sample, however, a resonant design using a tunable resonator is much more sensitive. While apparently a simple problem, designing a broadly tunable, high-Q electrical resonator is non-trivial. One solution is to use a mechanically tuned "loop-gap" resonator. The loop-gap resonator is especially effective in paramagnetic resonance experiments because of the combination of high-Q and small volume [47-51]. In a new design, the present experiment used piezoelectric tuning of the loop-gap resonator, shown in Figure 3.

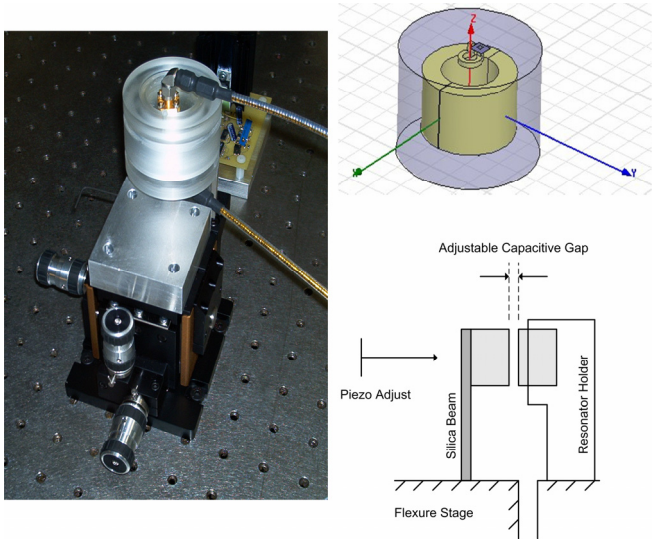

Figure 3. Mechanically Tuned Loop-Gap Resonator: Flexure Stage, Perspective view of loop gap resonator, and side-view showing piezo adjustment of capacitive gap

This design achieved octave tuning from 1-2 GHz, and a loaded-Q of approximately 300 with 2dB insertion loss. The paramagnetic resonance measurements were made using a transmission coupled resonator. Coupling was achieved using small magnetic loops, for complete details and fabrication, refer to [34]. An important shortcoming of the mechanical design using a cantilevered beam is sensitivity to acoustics, including sound generated by the Helmholtz coils.

Paramagnetic resonance may be detected as a change in the resonant frequency and quality factor of an electrical resonator which contains a paramagnetic sample. The phase change introduced by the paramagnetic sample to an RF carrier coupled through the resonator is (CGS units) [34]:

$$\Delta\theta = -4\pi\eta Q_L \chi' \qquad (7)$$

In Equation 7, η is the fill factor, which is the ratio of the magnetic energy stored in the sample to the total magnetic energy stored in the electrical resonator, Q_L is the loaded-Q of the loop-gap resonator, and χ' is the dispersive component of the magnetic susceptibility. If the paramagnetic resonance frequency is modulated using a Zeeman field, the phase-modulation sideband power introduced to the RF carrier is approximately:

$$P = 20\log_{10} 4\pi\eta Q_L \chi' \qquad (8)$$

For example, if the fill factor is ¼, the loaded-Q is 300, and the resonant magnetic susceptibility is 0.72×10^{-6}, the

sideband power is approximately -64 dBc. The carrier power used in the experiments was in the range of ~ 5 dBm.

C. *Frequency Discriminator and Zeeman-Modulation*

The phase modulation introduced by paramagnetic resonance is detected using a frequency-discriminator arrangement, shown in Figure 4. The frequency discriminator consists of a 90º hybrid or power splitter, transmission coupled loop-gap resonator, phase adjuster, and phase detector (e.g., mixer in quadrature).

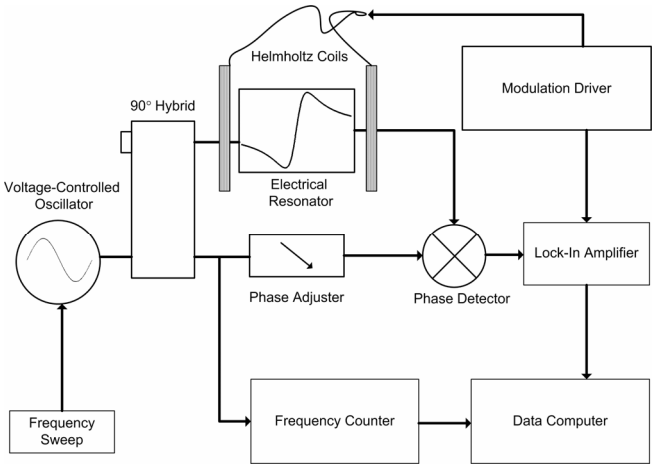

Figure 4. Zero-Field Paramagnetic resonance spectrometer

Helmholz coils are used to generate the Zeeman field, which is modulated using the bidirectional square-wave described in [41-44], with lock-in detection at the second harmonic. The modulation frequency was ~ 5 kHz. In the measurements described in the next section, the voltage-controlled oscillator is swept in the range of 1000 – 1200 MHz, and the output from the lock-in detector is recorded.

The sensitivity of the present experiments (SNR ~ 60dB, 1Hz BW) is limited by vibrations of the mechanically tuned resonator and the phase noise of the swept voltage-controlled oscillator. However, with improved design, frequency discriminator measurements limited by the thermal noise floor are feasible, using techniques such as carrier suppression [52-55]. Complete details of the spectrometer design are described in [34].

V. Measurement Results

A measured zero-field paramagnetic spectrum of a sample of magnesium oxide containing both vanadium and manganese is shown below in Figure 5. The modulation field was approximately 12 Gauss. The red curve is the measured spectrum and the blue curve is a calculation. We can see that the basic features of the calculated and measured spectrum are the same. The zero-field measurement allows for a more precise determination of the hyperfine coupling, which is seen to be approximately 1% lower than the published value determined from high-field measurements [30].

The apparent linewidth is probably due to the effect of the S^3 term in the more general Hamiltonian [32], which means that the different transitions in the $F = 4$ to $F = 5$ manifold are not exactly degenerate at zero field. These additional terms may also explain the asymmetry of the $F = 4$ to $F = 5$ transition at 1113 MHz. The resonance at 1180 MHz is due to Mn^{++}/MgO.

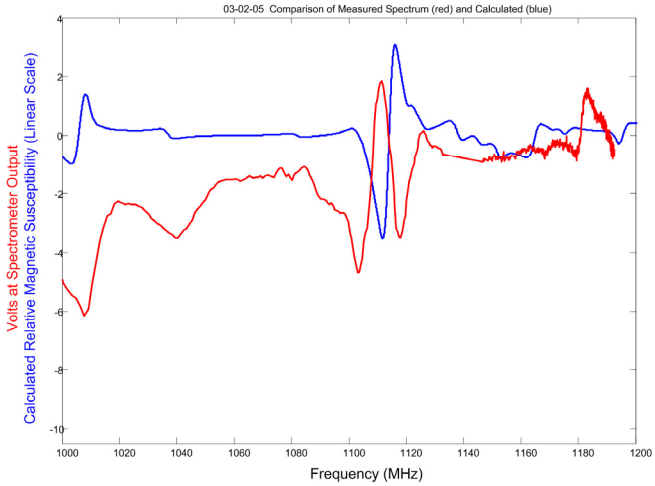

Figure 5. Measured Spectrum for Mn^{++} and V^{++} in Magnesium Oxide

The Zeeman measurement shown below in Figure 6 is for a vanadium doped magnesium oxide sample in a static magnetic field of approximately 50 Gauss, with the RF field polarized parallel to the Zeeman field. The modulation field used in the measurement was approximately 5 Gauss. The measurement validates the fact the for V^{++}/ MgO system, the dipolar linewidth scales with the Zeeman sensitivity, as described by (4). The measured linewidth of the $m_F = \pm 1$ transitions is half the linewidth of the $m_F = \pm 2$ transitions, and the $m_F = \pm 3$ and ± 4 transitions are seen to be even broader, in accordance with the theory. The linewidths seen in the figure are limited by the modulation amplitude; the actual linewidth limited by dipolar broadening is narrower than what is shown in the figure. The magnetic field independent $m_F = 0$ is barely observed in this particular measurement because of the small modulation field.

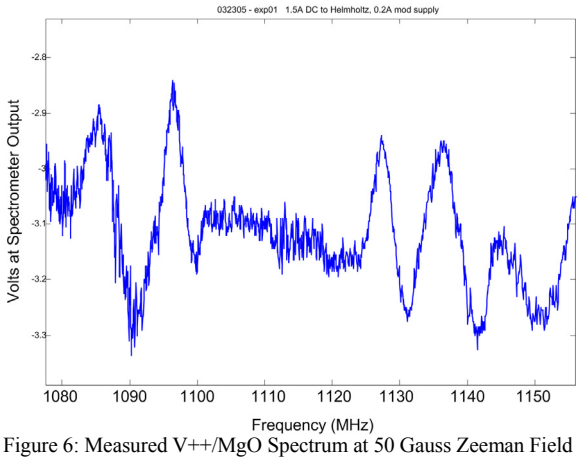

Figure 6: Measured V++/MgO Spectrum at 50 Gauss Zeeman Field

Zeeman modulation of the first-order magnetic field independent line would require audio magnetic fields on the order of 100 Gauss to adequately shift the line. Generating audio magnetic fields of 100 Gauss has significant power requirements. A spectrometer design using frequency modulation, similar to conventional atomic clocks, would be a better technique to measure the magnetic field independent $m_F = 0$ to $m_F = 0$ transition.

VI. Paramagnetic Resonance Linewidths

The dominant line broadening mechanism in solid-state magnetic resonance measurements is typically inhomogeneous broadening of the magnetic resonance transitions due to the random distribution of the local magnetic field within the crystal. Each site in the crystal lattice is surrounded by a different distribution of paramagnetic ions. The sum of the magnetic fields due the magnetic moments of the surrounding paramagnetic ions results in a random distribution of magnetic fields within the crystal, and therefore a broadening of the magnetic resonance transitions in proportion to the Zeeman sensitivity.

The theory of dipolar broadening in paramagnetic crystals is well established [56, 57]. A series of papers by de Biasi give thorough experimental validation for the dipolar broadening theory in magnesium oxide and related oxide crystals doped with Cr^{3+}, Mn^{++}, and other ions [58-63]. At higher doping concentrations (on the order of 0.1-1 mol %), there are a substantial number of exchange coupled pairs, which assuming anti-ferromagnetic coupling, have zero-magnetic moment, and do not contribute to the line broadening or resonance signals. The theory by de Biasi accounts for this effect [58]. The dipolar broadening for Cr^{3+}/MgO, which is isoelectronic with V^{++}, is given by:

$$\Delta H_{pp}(C) = \Delta H_{dd} = 6.23 f (1 - 0.01 f)^{54} \qquad (9)$$

In (9), the width of the magnetic field distribution is in mT, and f is the doping concentration in mol%. At zero field, the theory needs slight modification to take into account the different Landé factors of the zero-field eigenstates, which results in an additional factor of ½ [34]. At 1 mol% V^{++} doping, the zero-field width from (9) is ½ × 36.2 Gauss, which multiplying by the Zeeman sensitivity (4), corresponds to a zero-field resonance width of 5.1 MHz for $m_F = \pm 1$ transitions.

The upshot of this analysis is that it appears feasible to use much higher doping concentrations (~0.1-1%) while still measuring narrow $m_F = 0$ lines, which are independent of dipolar broadening to first order. Intense paramagnetic resonance transitions, with linewidths of at most 1 MHz, and possibly narrower, should be measurable even at high doping concentrations. The narrowing of magnetic field independent transitions of vanadyl ions in ammonium sulphate was previously reported by Bramley and Strach [43].

The actual resonance width of the $m_F = 0$ to $m_F = 0$ transitions would depend on additional inhomogeneous broadening mechanisms, such as stress distribution within the crystals [67], and the spin-lattice relation time T1. It would seem possible that the stress distribution within the crystal can be optimized through proper manufacturing and annealing, possibly resulting in very narrow resonance lines (~100 kHz wide). A conservative estimate of the atomic Q_A for the magnetic field independent transition is 1000. By assuming sensitivity in the range of 100 dB for an improved instrument, short-term stability in the range of 10^{-8} to 10^{-9} is predicted according to (1). The temperature coefficient of the hyperfine constant is on the order of ppm/ ºC [68].

VII. Conclusion

The paper has presented a new type of microwave passive atomic frequency reference, which is entirely solid-state and uses only low-cost electronic components. We have shown that vanadium doped magnesium oxide exhibits narrow hyperfine resonances at room temperature, which can be measured with high sensitivity using a simple paramagnetic resonance spectrometer.

We also predict that the $m_F = 0$ to $m_F = 0$ magnetic field independent transitions is unaffected by dipolar broadening, i.e., by the dominant mechanism for line broadening in solids. This implies that we may increase the doping concentration, and thereby the signal intensity, without broadening the $m_F = 0$ transition to first-order. Finally, validation of the short-term stability estimates and an understanding of mechanisms affecting long-term stability are topics for future work.

Acknowledgment

The authors thank Richard Bramley for generously discussing his earlier zero-field paramagnetic resonance work. Thanks also to James White for assisting with the resonator fabrication, and to Philip Feng for annealing the magnesium oxide crystals.

References

[1] L. L. Lewis, "An introduction to frequency standards," *Proceedings of the IEEE,* vol. 79, no. 7, pp. 927-935, July 1991.

[2] S. Knappe *et al.*, "A microfabricated atomic clock," *Applied Physics Letters,* 85, pp. 1460, 2004.

[3] L. Liew *et al.*, "Microfabricated alkali atom vapor cells," *Applied Physics Letters,* 84, pp. 2694, 2004.

[4] H. C. Nathanson and I. Liberman, United States Patent 6,570,459, "Physics Package Apparatus for an Atomic Clock," Northrop Grumman Corporation, Los Angeles, CA, May 27, 2003.

[5] J. Kitching *et al.*, "Miniature vapor-cell atomic-frequency references," *Applied Physics Letters*, 81, pp. 553, 2002.

[6] J. Kitching, "Compact atomic clock based on coherent population trapping," *Electronics Letters*, vol. 37, no. 24, pp. 1449-1451, November 2001.

[7] J. Vanier *et al.*, "The coherent population trapping passive frequency standard [Rb example]," *IEEE Trans. on Instrumentation and Measurement,* vol. 52, no. 2, pp. 258-262, April 2003.

[8] J. Vanier *et al.*, "Atomic Clocks Based on Coherent Population Trapping: Basic Theoretical Models and Frequency Stability," *Proc. IEEE International Frequency Control Symposium*, pp. 2-15, 2003.

[9] M. Zhu, "High Contrast Signal in Coherent Population Trapping Based Atomic Frequency Standard Application," *Proc. IEEE International Frequency Control Symposium*, pp. 16-21, 2003.

[10] S. Knappe *et al.*, "Atomic Vapor Cells for Miniature Frequency References," *Proc. IEEE International Frequency Control Symposium*, pp. 31-32, 2003.

[11] J. Vanier, "Coherent Population Trapping for the Realization of a Small, Stable, Atomic Clock," *Proc. IEEE International Frequency Control Symposium*, pp. 424-434, 2002.

[12] J. Kitching, S. Knappe and L. Holberg, "Performance of Small Scale Frequency References," *Proc. IEEE International Frequency Control Symposium*, pp. 442-446, 2002.

[13] J. Kusters and J. Vig, "Hysteresis in Quartz Resonators – A Review," *IEEE Trans. on Ultrasonics, Ferroelectrics, and Frequency Control*, vol. 38, no.3, pp.281-289, May 1991.

[14] F. Walls and J. Vig, "Fundamental Limits on the Frequency Stabilities of Crystal Oscillators," *IEEE Trans. on Ultrasonics, Ferroelectrics, and Frequency Control*, vol. 42, no. 4, pp. 576-589, July 1995.

[15] R. Filler and J. Vig, "Long-Term Aging in Oscillators," *IEEE Trans. on Ultrasonics, Ferroelectrics, and Frequency Control*, vol. 40, no. 4, pp.387-394, July 1993.

[16] Y. Yong and J. Vig, "Modeling Resonator Frequency Fluctuations Induced by Absorbing and Desorbing Surface Molecules," *IEEE Trans. on Ultrasonics, Ferroelectrics, and Frequency Control*, vol. 37, no. 6, pp. 543-550, November 1990.

[17] Y. Yong and J. Vig, "Resonator Surface Contamination – A Cause of Frequency Fluctuations?," *IEEE Trans. on Ultrasonics, Ferroelectrics, and Frequency Control*, vol. 36, no. 4, pp. 452-458, July 1989.

[18] R. Filler and J. Vig, "Resonators for the Microcomputer Compensated Crystal Oscillators," *Proc. 43rd Ann. Symposium on Frequency Control*, pp. 1-15, 1989.

[19] M. Bloch *et al.*, "Low Power Timekeeping," *Proc. 43rd Ann. Symposium on Frequency Control,* pp. 34-36, 1989.

[20] Garland *et al.*, United States Patent 3,431,392, "Internally Heated Crystal Devices," Hughes Company, Culver City, CA, March 4, 1969.

[21] I. Abramson and A. Dikidzhi, "Improvement of Characteristics of Quartz Resonator-Thermostate with Direct Heating Piezoelement," *IEEE Frequency Control Symposium*, pp. 499-504, 1992.

[22] I. Abramson, "Internal Heated Quartz Resonator with Low Sensitivity to an Acceleration," *IEEE International Frequency Control Symposium*, pp. 838-842, 1995.

[23] I. Balaz and M. Minarik, "Towards and OCXO with Infrared Heater," *IEEE International Frequency Control Symposium*, pp. 674-680, 1996.

[24] T. J. Lynch and J. R. Vaccaro, "Ultrafast Warm-Up Rubidium References," *Proc. IEEE International Frequency Control Symposium*, pp. 993-1001, 1996.

[25] Stephen D. LaLumondiere, Steven C. Moss, and James C. Camparo, "A "Space Experiment" Examining the Response of a Geosynchronous Quartz Crystal Oscillator to Various Levels of Solar Activity," *IEEE Trans. on Ultrasonics, Ferroelectrics, and Frequency Control*, 50, 210, 2003.

[26] J. R. Pilbrow, Transition Ion Electron Paramagnetic Resonance, Oxford: Clarendon, 1990.

[27] A. Abragam and B. Bleaney, Electron Paramagnetic Resonance of Transition Ions, Oxford: Clarendon, Oxford, 1970.

[28] Charles P. Poole, Jr. and Horacia A. Farach, Handbook of Electron Spin Resonance, Volume 1 and 2, Springer-Verlag New York, Inc., 1999.

[29] Chales P. Poole, Jr., Electron Spin Resonance: A Comprehensive Treatise on Experimental Techniques, Wiley, 1983.

[30] W. Low, "Paramagnetic Resonance Spectra of Some Ions in the 3d and 4f Shells in Cubic Crystalline Fields," *Phy. Rev.*, vol. 101, pp. 1827, 1956.

[31] J.E. Wertz, J. W. Orton, and P. Auzins, "Spin Resonance of Point Defects in Magnesium Oxide," *J. Appl. Phys.*, vol. 33, no. 1, pp. 322-328, 1962.

[32] R. S. de Biasi, "Influence of the S^3 Term on the EPR Spectrum of Cr^{3+} in Cubic Symmetry Sites in MgO," *Journal of Magnetic Resonance*, vol. 44, pp. 479-482, 1981.

[33] E. U. Condon & G. H. Shortley, *The Theory of Atomic Spectra*, Cambridge University Press, pp. 63, 1963.

[34] Christopher White, "A Solid-State Atomic Frequency Standard," Ph. Thesis, Caltech 2005.

[35] A. Yariv, *Quantum Electronics*, Wiley, 1st ed., 1967.

[36] M. D. Sturge, "Optical Spectrum of Divalent Vanadium in Octahedral Coordination," *Physical Review*, vol. 130, no. 2, pp. 639-646, April 1963.

[37] D. H. Dickey and J. E. Drumheller, "Forbidden Hyperfine Transitions in the Electron Paramagnetic Resonance of V^{++} in MgO," *Physical Review*, vol. 161, no. 2, pp. 279-282, September 1967.

[38] W. H. Gourdin, W. D. Kingery, and J. Driear, "The Defect Structure of MgO Containing Trivalent Cation Solutes: The Oxidation-Reduction Behavior of Iron," *J. Mater. Sci.*, vol. 14, pp. 2074-82, 1979.

[39] K.N. Woods and M.E. Fine, "Nucleation and Growth of Magnesioferrite in MgO Containing 0.9 % Fe^{3+}," *J. Am. Ceram. Soc.*, vol. 52, no. 4, pp. 186-8, 1969.

[40] J.S. Thorp, A.R. Skinner and A.S. Al-Hawery, "Magnesiochromite Formation and EPR Linewidths in Cr/MgO," Journal of Magnetism and Magnetic Materials 82 (1989) 277-286.

[41] Christopher D. Delfs and Richard Bramley, "Zero-field electron magnetic resonance spectra of copper carboxylates," *J. Chem. Phys.*, vol. 107, pp. 8840, 1997.

[42] Christopher D. Delfs and Richard Bramely, "The zero-field ESR spectrum of a copper dimmer," *Chemical Physics Letters*, vol. 264, pp. 333, 1997.

[43] Richard Bramley and Steven J. Strach, "Zero-Field EPR of the Vanadyl Ion in Ammonium Sulfate," *J. of Magnetic Resonance*, vol. 61, pp. 245, 1985.

[44] Richard Bramley and Steven J. Strach, "Electron Paramagnetic Resonance Spectroscopy at Zero Magnetic Field," *Chem. Rev.*, vol. 83, pp. 49-82, 1983.

[45] Cole, T. Kushida, T., and Heller, H. C., "Zero-Field Electron Magnetic Resonance in Some Inorganic and Organic Radicals," *J. Chem. Phys.*, vol. 38, pp. 2915, 1963.

[46] P. R. Solomon, "Relaxation of Mn^{2+} and Fe^{3+} Ions in Magnesium Oxide," *Phys. Rev.*, vol. 152, no. 1, December 1966.

[47] W. Piasecki, W. Froncisz, and James S. Hyde, "Bimodal loop-gap resonator," *Rev. Sci. Instrum.*, 67, 1896, 1996.

[48] S. Pfenninger, W. Froncisz, J. Forrer, J. Luglia, and James S. Hyde, "General Method for Adjusting the Quality Factor of EPR resonators," *Rev. Sci. Instrum.*, 66, 4857, 1995.

[49] T. Christides, W. Froncisz, T. Oles, James S. Hyde, "Probehead with Interchangeable Loop-gap Resonators and RF Coils for Multifrequency EPR/ENDOR," *Rev. Sci. Instrum.*, 65, 63, 1994.

[50] W. Froncisz and James S. Hyde, "The Loop-gap Resonator: A New Microwave Lumped Circuit ESR Sample Structure," *J. Magnetic Resonance*, 47, 515, 1982.

[51] W. N. Hardy and L. A. Whitehead, "Split-ring resonator for use in magnetic resonance from 200-2000 MHz," *Rev. Sci. Instrum.*, 52, 213, 1981.

[52] Eugene N. Ivanov, M. E. Tobar, R. A. Woods, "Microwave Interferometry: Application to Precision Measurements and Noise

Reduction Techniques," *IEEE Trans. on Ultrasonics, Ferroelectrics, and Frequency Control*, 45, 1526, 1998.

[53] Eugene N. Ivanov, Micheal E. Tobar, Richard A. Woode, "Applications of Interferometric Signal Processing to Phase-Noise Reduction in Microwave Oscillators," *IEEE Trans. on Microwave Theory and Techniques*, 46, 1537, 1998.

[54] F. L. Walls, "Suppressed Carrier Based PM and AM Noise Measurement Techniques," *Proc. IEEE International Frequency Control Symposium*, pp. 485-492, 1997.

[55] E. N. Ivanov, M. E. Tobar and R. A Woode, "Advanced Phase Noise Suppression Technique for Next Generation of Ultra-Low Noise Microwave Oscillators," *Proc. IEEE International Frequency Control Symposium*, pp. 314-320, 1995.

[56] J. H. Van Vleck, "The Dipolar Broadening of Magnetic Resonance Lines in Crystals," *Physical Review*, vol. 74, no. 9, pp.1168-1183, Nov. 1948.

[57] C. Kittel and E. Abrahams, "Dipolar Broadening of Magnetic Resonance Lines in Magnetically Diluted Crystals," *Physical Review*, vol. 90, no. 2, pp. 238-239, Apr. 1953.

[58] R.S. de Biasi and A A R Fernandes, "The ESR linewidth of dilute solid solutions," *J. Phys. C: Solid State Phys.*, 16 (1983) 5481-5489.

[59] R. S. de Biasi and A. A. R. Fernades, "Measurement of Small Concentrations of Cr and Mn in MgO Using Electron Spin Resonance," *Communications of the American Ceramic Society*, September 1984 pp. C-173 – C-175.

[60] R. S. de Biasi and M. L. N. Grillo, "Influence of manganese concentration on the ESR spectrum of Mn^{2+} in CaO," *Journal of Alloys and Compounds*, 282, (1999), pp. 5-7.

[61] R.S. de Biasi, M.L.N. Grillo, "Influence of manganese concentration on the ESR spectrum of Mn^{2+} in SrO," *Journal of Alloys and Compounds* 290 (1999) 22-24

[62] R. S. de Biasi, and M. L. N. Grillo, "Influcence of copper concentration on the ESR spectrum of Cu^{2+} in MgO," *Journal of Alloys and Compounds*, 302, 2000, pp. 26-28.

[63] R. S. de Biasi and M. L. N. Grillo, "Influence of gadolinium concentration on the ESR spectrum of Gd^{3+} in SrO," *Journal of Alloys and Compounds*, 337, 2002, pp. 30-32.

[64] J.S. Thorp, A.R. Skinner and A.S. Al-Hawery, "Magnesiochromite Formation and EPR Linewidths in Cr/MgO," Journal of Magnetism and Magnetic Materials 82 (1989) 277-286.

[65] J.S. Thorp, M.D. Hossain, "ESR line broadening in Cr^{3+}/MgO at liquid helium temperatures," Journal of Materials Science 15 (1980) 3041-3046.

[66] J.S. Thorp, M.D. Hossain, L.J.C. Bluck, "Electron spin resonance linewidths of Cr^{3+} in magnesium oxide," Journal of Materials Science 14 (1979) 2853-2858.

[67] E.R. Feher, "Effect of Uniaxial Stresses on the Paramagnetic Spectra of Mn^{2+} and Fe^{3+} in MgO," Physical Review, Volume 136, Number 1A, 5 October 1964, A145-160.

[68] Walter M. Walsh, Jr., Jean Jeener, and N. Bloembergen, "Temperature-Dependent Crystal Field and Hyperfine Interactions," *Phys. Rev.*, vol. 139, pp. A 1338, 1965.